The electrochemical behavior shows that one product is the acetonitrile complex; another may be the ethylamine complex, but this has not been proven.

We set out to measure the deprotonation equilibrium between an η^2-iminium complex and chose to measure the corresponding imine complex equilibrium quotient for the imine derived from acetone, earlier work[4] having shown that this is much more stable than **7**.

$$[Os(NH_3)_5(\eta^2\text{-}(CH_3)_2C{=}NH_2)]^{3+} = [Os(NH_3)_5(\eta^1\text{-}(CH_3)_2C{=}NH)]^{2+} + H^+ \quad (1)$$

To this end, we recorded the absorption spectrum of **5** in a series of aqueous buffer solutions covering the range pH = 13 to pH = 0. In each of these extremes, the absorption is independent of pH over a range. In 0.1 M NaOH, **5** shows an absorption maximum at 212 nm ($\epsilon = 3.6 \times 10^4$ M^{-1} cm^{-1}) but at pH = 8 and lower, there is no significant absorption in this wavelength region. Measurements at room temperature in the intermediate pH range yielded for the pK_a of the acid $[Os(NH_3)_5(\eta^2\text{-}(CH_3)_2C{=}NH_2)]^{3+}$ the value of 10.3 ± 0.2.

Discussion

There are only a few examples of complexes in which an iminium cation, at least singly protonated on the nitrogen, is bound to a metal atom.[11] Our review of the literature suggests that in no case has the iminium ligand been generated by protonation of the imine nor has an equilibrium of the type represented by (1) been reported. Our work with the imine derived from acetone sets only a lower limit on the pK_a for reaction 2. The pK_a value

$$[Os(NH_3)_5(\eta^2\text{-}(CH_3)_2C{=}NH_2)]^{3+} \rightarrow [Os(NH_3)_5(\eta^2\text{-}(CH_3)_2C{=}NH)]^{2+} + H^+ \quad (2)$$

for reaction 2 will be increased over that for reaction 1 by the pK for (3) (the sum of reactions 1 and 3 is reaction 2).

$$[Os(NH_3)_5(\eta^1\text{-}(CH_3)_2C{=}NH)]^{2+} = [Os(NH_3)_5(\eta^2\text{-}(CH_3)_2C{=}NH)]^{2+} \quad (3)$$

The high proton affinity of an η^2-bound imine suggests that conversion of such imines to η^2-iminium derivatives by the action of carbonium ion donors can be realized.

Not understood is the difference in the action of the reducing agent Mg(0) ion on the one hand and zinc amalgam on the other. A possibility is that Mg rapidly scavenges protons, so that the reduction to imine, which requires protons, is disfavored. Nor is it at all clear why the yield of the iminium adduct is much reduced when the reaction medium changes from almost pure acetonitrile to water. It is unlikely that this behavior is attributable to a lower driving force for the reaction in water compared to acetonitrile. The 2e reduction of the acetonitrile complex to the iminium is represented by the equation

$$Zn + 3H_2O + [Os(NH_3)_5(CH_3CN)]^{2+} = Zn(OH)_2 + [Os(NH_3)_5(CH_3{-}CH{=}NH_2)]^{3+} + OH^-$$

The activity of the solids is unaffected by a change in solvent. Both because water is a reactant and because the ionic products are expected to be stabilized relative to the ionic reactant when water replaces acetonitrile as the solvent, the driving force is expected to be greater in water. It seems rather certain that the effect of the solvent change on the chemistry is a matter of mechanism rather than equilibrium stability.

Acknowledgment. The research was supported by National Science Foundation Grant No. CHE8511658. It is a pleasure also to acknowledge helpful discussions with Professor Helmut Fischer, University of Konstanz. T.H. acknowledges Shin-Etsu Chemical Co., Ltd., for partial financial support.

(11) (a) Matsumoto, M.; Nakatsu, K.; Tani, K.; Nakamura, A.; Otsuka, S. *J. Am. Chem. Soc.* **1974**, *96*, 6777. (b) Brunner, H.; Wachter, J.; Schmidbauer, J. *Organometallics* **1986**, *5*, 2212.

Contribution from the Departments of Chemistry, The University of North Carolina at Charlotte, Charlotte, North Carolina 28223, and The University of North Carolina at Chapel Hill, Chapel Hill, North Carolina 27514

MLCT-dd Energy Gap in Pyridyl-Pyrimidine and Bis(pyridine) Complexes of Ruthenium(II)

D. Paul Rillema,*,† Charles B. Blanton,† Randy J. Shaver,† Donald C. Jackman,† Massoud Boldaji,† Stephanie Bundy,† Laura A. Worl,‡ and Thomas J. Meyer*,‡

Received October 10, 1991

The photophysical and photochemical properties of a series of 2-(2′-pyridyl)pyrimidine and bis(pyridine) polypyridyl complexes of ruthenium(II) are described. The temperature dependences of the emission decay were fit to the equation $1/\tau(T) = k_1 + k_2 \exp(-\Delta E_2/RT)$. The values of k_1 ranged from 7.1×10^5 to 8.7×10^6 s^{-1}, k_2 ranged from 9×10^6 to 3×10^{17} s^{-1}, and ΔE_2 ranged from 428 to 4776 cm^{-1}. A plot of ln k_2 vs ΔE_2, known as a Barclay-Butler plot, was linear with a slope of 2.9×10^{-3} cm and a y intercept of 5.9. The study demonstrates the usefulness of excited-state parameters for assessing the photolability and/or stability of ruthenium(II) pyridyl complexes. It has also led to the design of the photostable core "$[Ru(bpy)(bpz)]^{2+}$" which may be of value in the design of molecular assemblies.

Introduction

A number of studies on the properties of polypyridyl complexes, in our work[1-4] and the work of others,[5-13] have focused attention on the problem of photosubstitution. The mechanism of the reaction is thought to involve ligand loss and formation of a five-coordinate intermediate.[7] There is evidence that photosubstitution follows a general pattern based on the energy gap between the ^{3}MLCT state and the ground state.[2] In a recent study, the logarithm of the quantum yield for photosubstitution was found

†The University of North Carolina at Charlotte.
‡The University of North Carolina at Chapel Hill.

(1) (a) Durham, B.; Walsh, J. L.; Carter, C. L.; Meyer, T. J. *Inorg. Chem.* **1980**, *19*, 850. (b) Durham, B.; Caspar, J. V.; Nagle, J. K.; Meyer, T. J. *J. Am. Chem. Soc.* **1982**, *104*, 4803.
(2) Allen, G. H.; White, R. P.; Rillema, D. P.; Meyer, T. J. *J. Am. Chem. Soc.* **1984**, *106*, 2613.
(3) Rillema, D. P.; Taghdiri, D. G.; Jones, D. S.; Keller, C. D.; Worl, L. A.; Meyer, T. J.; Levy, H. A. *Inorg. Chem.* **1987**, *26*, 578.
(4) Ross, H. B.; Boldaji, M.; Rillema, D. P.; Blanton, C. B.; White, R. P. *Inorg. Chem.* **1989**, *28*, 1013.

0020-1669/92/1331-1600$03.00/0

to vary linearly with the MLCT energy gap for a given series of complexes based on the ligand having the lowest π^* energy level.[4]

Strategies to eliminate the dd state from its role in the excited-state manifolds of these complexes have involved turning to Os(II), where 10 *Dq* is approximately 30% greater than for Ru(II),[14] and to mixed-ligand chelates of ruthenium(II), where the ^{3}MLCT level can be brought below the dd state by controlling the energy of the π^* acceptor levels.[2,3] The further development of these strategies for Ru(II) is a matter for synthesis, since the chemistry of polypyridyl complexes of Ru(II) is well advanced and techniques are available to prepare complexes which could serve as components in complex molecular assemblies for photoinduced electron or energy transfer.

Here we turn to 2-(2′-pyridyl)pyrimidine and bis(pyridine) complexes as potential models for more complex systems containing electron- or energy-transfer donors or acceptors based on pyridine binding to Ru(II). We have followed an earlier lead[15] in the design of "photostable" mixed-ligand chelates with the hopes of extending the earlier finding to bis(pyridyl)-type complexes in order to minimize problems arising from photosubstitution.

Experimental Section

Materials. The ethanol used in the excited-state measurements was freshly distilled over MgI_2. Tetraethylammonium chloride (TEAC1), purchased from Aldrich, was purified by the procedures of Unni, Elias, and Schift[16] and stored in a vacuum oven. Tetrabutylammonium hexafluorophosphate (TBAH) was purchased as electrometric grade from Southwestern Analytical and stored in a vacuum oven before use. The acetonitrile and the methylene chloride were of spectrophotometric grade and dried over 4-Å molecular sieves before use in the electrochemistry experiments. Methanol was used as received from Burdick and Jackson. All other reagents were purchased as reagent grade and used without further purification.

Preparation of Compounds. The preparations of $Ru(bpy)_2Cl_2\cdot 2H_2O$[17] and $Ru(bpy)Cl_4$[18] followed previously reported procedures. The complexes $[Ru(bpz)_2(py)_2]^{2+}$, $[Ru(bpm)_2(py)_2]^{2+}$, $[Ru(dmb)_2(py)_2]^{2+}$, and $[Ru(bpz)(bpy)(py)_2]^{2+}$ were available as $CF_3SO_3^-$ or PF_6^- salts from a previous study.[4] The complex $Ru(bpy)_2CO_3\cdot 2H_2O$ was prepared according to a published literature procedure.[19] 2-(2′-Pyridyl)pyrimidine was prepared according to a method previously reported by Lafferty and Case:[20] mp 186–187 °C (lit.[20] 188–190 °C); ^{1}H NMR ($CDCl_3$) 8.80 (d, J = 4 Hz, 2 H), 8.73 (d, J = 4 Hz, 1 H), 8.41 (d, J = 7.5 Hz, 1 H), 7.74 (td, J = 8 Hz, 2.2 Hz, 1 H), 7.28 (dd, J = 8, 5.6 Hz, 1 H), 7.20 (t, J = 5 Hz, 1 H).

The ligand abbreviations are bpz (2,2′-bipyrazine), bpm (2,2′-bipyrimidine), dmb (4,4′-dimethyl-2,2′-bipyridine), bpy (2,2′-bipyridine), py (pyridine), and pypm (2-(2′-pyridyl)pyrimidine).

$[Ru(bpy)_2(py)_2](CF_3SO_3)_2$. The compound was prepared by adding 0.109 g (2.3×10^{-4} mol) of $Ru(bpy)_2CO_3\cdot 2H_2O$ to 2 mL of trifluoromethanesulfonic acid in a 10-mL round-bottom flask. The solution was heated to reflux for ~1 h, during which time the color of the solution changed from orange to blue. The solution was allowed to cool to room temperature, and then it was added to a beaker containing 200 mL of stirring diethyl ether. The blue precipitate that formed was collected on a fritted disk filter by vacuum suction. Then it was added to a 50-mL flask containing 30 mL of pyridine, which caused a red color to develop immediately. The red solution was protected from light, placed under N_2, and heated at reflux for 2 h, during which time an orange precipitate formed. The solution was cooled, and the precipitate was collected by filtration, washed with diethyl ether, and dried under vacuum. The resulting orange precipitate was dissolved in a minimum amount of acetonitrile, and the solution was chromatographed on a neutral alumina column 7.0 cm in length and 6.0 cm in diameter. The column had previously been developed with acetonitrile, and acetonitrile served as the eluent. The middle fraction was collected, filtered to remove insoluble impurities, and concentrated on a rotary evaporator. The concentrated solution was added to an excess of swirling diethyl ether to precipitate the purified complex. It was isolated by vacuum filtration and dried in a vacuum oven at 25 °C. Anal. Calc: C, 44.14; H, 3.03; N, 9.62. Found: C, 44.19; H, 3.01; N, 9.66.

$[Ru(2\text{-}(2'\text{-pyridyl})pyrimidine)_3](PF_6)_2$. A 25-mL round-bottom flask was charged with 0.10 g (4.8×10^{-4} mol) of $RuCl_3$ and 0.20 g (1.27×10^{-3} mol) of 2-(2′-pyridyl)pyrimidine suspended in 10 mL of ethylene glycol. The reaction mixture was allowed to reflux for 30 min, during which time it changed color from green to a dull orange. The solution was cooled, filtered, and sufficient water was added to double the volume. A saturated aqueous NH_4PF_6 solution was added until precipitation of the product appeared to be complete. The suspension was filtered by vacuum filtration, and the solids were washed with cold water and with diethyl ether to remove the ethylene glycol. The product was dissolved in a minimal amount of acetonitrile, and the solution was chromatographed over a neutral alumina column 10 cm in length and 2.5 cm in diameter. The column was developed with acetonitrile and eluted with a 3:1 mixture of acetonitrile:acetone as the mobile phase. Three bands were observed. The first was orange; the second was red; and the third band was dark gray and was retained at the top of the column. The first band, found to be the desired product by cyclic voltammetry, was collected and filtered to remove insoluble impurities; then the solvent was removed with a rotary evaporator. The product was then redissolved in a minimal amount of acetonitrile and reprecipitated by addition into cold, swirling diethyl ether. The product was collected and dried in the vacuum oven. Yield: 0.23 g (54.5%). Anal. Calc: C, 36.83; H, 2.63; N, 14.32. Found: C, 37.38; H, 2.87; N, 13.86.

$[Ru(bpy)(2\text{-}(2'\text{-pyridyl})pyrimidine)_2](PF_6)_2$. A 25-mL round-bottom flask was charged with 0.16 g (1.02×10^{-3} mol) of 2-(2′-pyridyl)pyrimidine and 0.11 g (2.76×10^{-4} mol) of $Ru(bpy)Cl_4$ suspended in 15 mL of ethylene glycol. The solution was refluxed for 30 min, during which time the color of the solution changed from green to red. The solution was cooled to room temperature and filtered. The volume of the filtrate was doubled with water, and a saturated aqueous solution of NH_4PF_6 was added to precipitate the product. The precipitate was collected by vacuum filtration, washed with water, and then dissolved in a minimal amount of acetonitrile. The crude product was precipitated by addition to diethyl ether in order to remove the excess ethylene glycol, and the precipitate was collected by filtration. The resulting solid was chromatographed on a neutral alumina column 10 cm in length and 2.5 cm in diameter. The column was developed using acetonitrile, and the eluent was a 3:1 mixture of acetonitrile:acetone. The first fraction, determined by cyclic voltammetry to be the desired product, was collected and filtered. The solvent was then reduced to a volume of about 5–10 mL with a rotary evaporator. The product was precipitated by addition into cold, swirling diethyl ether, collected by filtration, and dried in a vacuum oven. Yield: 0.14 g (57.5%). Anal. Calc: C, 39.04; H, 2.57; N, 13.01. Found: C, 39.24; H, 2.63; N, 12.85.

$[Ru(bpy)_2(2\text{-}(2'\text{-pyridyl})pyrimidine)](CF_3SO_3)_2$. A 250-mL round-bottom flask was charged with 0.13 g (2.5×10^{-4} mol) of $Ru(bpy)_2Cl_2\cdot 2H_2O$ dissolved in 100 mL of acetone, and the solution was stirred for 15 min, after which 0.13 g (5.94×10^{-4} mol) of $Ag(CF_3SO_3)$ in 10 mL of acetone was added. The solution was allowed to reflux for 2 h, after which the precipitated AgCl was removed by filtration. To the filtrate was added 0.18 g (1.14×10^{-3} mol) of 2-(2′-pyridyl)pyrimidine in 10 mL of acetone, and the solution was refluxed for 2 h. The reaction mixture was filtered, and the solvent was reduced via the rotary evaporator to a volume of approximately 5 mL. The product was precipitated

(5) (a) Gleria, M.; Minto, F.; Beggiato, G.; Bortolus, P. *J. Chem. Soc., Chem. Commun.* **1978**, 285. (b) Jones, R. F.; Cole-Hamilton, D. J. *Inorg. Chim. Acta* **1981**, *53*, L3. (c) Fetterolf, M. L.; Offen, J. W. *Inorg. Chem.* **1987**, *26*, 1070.

(6) (a) Hoggard, P. R.; Porter, G. B. *J. Am. Chem. Soc.* **1978**, *100*, 1457. (b) Wallace, W. M.; Hoggard, P. E. *Inorg. Chem.* **1980**, *19*, 2141. (c) Fasano, R.; Hoggard, P. R. *Ibid.* **1983**, *22*, 566.

(7) (a) Van Houten, J.; Watts, R. J. *Inorg. Chem.* **1978**, *17*, 3381. (b) Watts, R. J. *J. Chem. Educ.* **1983**, *60*, 834.

(8) Kirchhoff, J. R.; McMillin, D. R.; Marnot, P. A.; Sauvage, J. P. *J. Am. Chem. Soc.* **1985**, *107*, 1138.

(9) (a) Wacholtz, W. M.; Auerbach, R. A.; Schmehl, R. H.; Ollino, M.; Cherry, W. R. *Inorg. Chem.* **1985**, *24*, 1758. (b) Wacholtz, W. F.; Auebach, R. A.; Schmehl, R. H. *Ibid.* **1986**, *25*, 227.

(10) (a) Pinnick, D. V.; Durham, B. *Inorg. Chem.* **1984**, *23*, 1440. (b) Pinnick, D. V.; Durham, B. *Ibid.* **1984**, *23*, 3842.

(11) Henderson, L. J.; Cherry, W. R. *Chem. Phys. Lett.* **1985**, *114*, 553.

(12) Kalyanasundaram, K. *J. Phys. Chem.* **1986**, *90*, 2285.

(13) Fetterolf, M. L.; Offen, J. W. *Inorg. Chem.* **1985**, *24*, 2755.

(14) (a) Kober, E. M.; Meyer, T. J. *Inorg. Chem.* **1984**, *23*, 3877. (b) Kober, E. M.; Marshall, J. L.; Dressick, W. J.; Sullivan, B. P.; Caspar, J. V.; Meyer, T. J. *Inorg. Chem.* **1985**, *24*, 2755.

(15) Rillema, D. P.; Allen, G.; Meyer, T. J.; Conrad, D. *Inorg. Chem.* **1983**, *22*, 1617.

(16) Unni, A. K. R.; Elias, L.; Schift, H. I. *J. Phys. Chem.* **1963**, *67*, 1216.

(17) Sprintschinik, G.; Sprintschinik, H. W.; Whitten, D. G. *J. Am. Chem. Soc.* **1976**, *98*, 2337.

(18) Krause, R. A. *Inorg. Chim. Acta* **1977**, *22*, 209.

(19) Johnson, E. C.; Sullivan, B. P.; Salmon, D. J.; Adeyemi, S. A.; Meyer, T. J. *Inorg. Chem.* **1978**, *17*, 2211.

(20) Lafferty, J. L.; Case, F. H. *J. Org. Chem.* **1967**, *32*, 1591.

Table I. Visible–UV Spectra of Ruthenium(II) Complexes[a]

complex	$d\pi \rightarrow \pi^*_1$	$d\pi \rightarrow \pi^*_2$	$\pi \rightarrow \pi^*$
$[Ru(bpm)_3]^{2+}$ [b]	454 (8.6×10^3)	362 (sh)	252 (4.9×10^4)
	418 (8.2×10^3)	332 (1.7×10^4)	
$[Ru(pypm)_3]^{2+}$ [c]	450 (2.1×10^4)	368 (1.5×10^4)	279 (1.0×10^5)
	429 (1.9×10^4	329 (1.8×10^4)	243 (5.5×10^4)
$[Ru(bpy)(pypm)_2]^{2+}$	447 (8.0×10^3)	321 (sh)	282 (3.4×10^4)
	435 (7.9×10^3)		246 (3.4×10^4)
$[Ru(bpy)_2(pypm)]^{2+}$	449 (1.1×10^4)	317 (sh)	285 (5.2×10^4)
	425 (sh)		257 (2.0×10^4)
			246 (2.3×10^4)
$[Ru(bpy)_3]^{2+}$	451 (1.4×10^4)	345 (6.5×10^3)	285 (8.7×10^4)
		323 (6.5×10^3)	250 (2.5×10^4)
			238 (3.0×10^4)

[a] In acetonitrile; $T = 23 \pm 1$ °C; λ_{max} in nm (error is ±1 nm); ϵ in parentheses, units in M^{-1} cm^{-1} (error is ±0.1). [b] From: Crutchley, R. S.; Lever, A. B. P. *Inorg. Chem.* **1982**, *21*, 2276. [c] Expanded from the data reported in ref 27.

by addition into diethyl ether and collected by vacuum filtration. The precipitate was chromatographed using a neutral alumina column with acetonitrile as the developer and a 3:1 acetonitrile:acetone mixture as the eluent. The first fraction was collected, and the solvent was reduced to a volume of about 5 mL. The solution was then reprecipitated by addition to diethyl ether. The product was collected and dried in a vacuum oven. Yield: 0.13 g (61.5%). Anal. Calc: C, 42.86; H, 2.67; N, 11.29. Found: C, 42.80; H, 2.72; N, 11.19.

Measurements. Visible–UV spectra were obtained on a Perkin-Elmer Model 3840 diode array spectrophotometer. Corrected solution emission spectra were obtained on an Spex Fluorolog spectrofluorometer. Cyclic voltammograms were obtained in methylene chloride or acetonitrile at a Pt-disk working electrode and a Pt-mesh counter electrode with 0.1 M tetrabutylammonium hexafluorophosphate (TBAH) as the supporting electrolyte. The reported potentials were versus a saturated sodium chloride calomel electrode (SSCE). These measurements were performed with a PAR 174 polarographic analyzer or the PAR 173 potentiostat in conjunction with a PAR 175 programmer and recorded with a YEW Model 3022 A4 *X–Y* recorder.

Photochemical quantum yield measurements were carried out in a nitrogen-degassed acetonitrile solution containing 1 mM TEACl. The procedure used was a modification of one previously reported.[2] A Photon Technology Inc. apparatus consisting of a PTI LPS200X 75-W photolysis system, an Oriel Model 77250 monochromator, and a cell holder mounted on an optical rail was used for the photolysis investigations. The cells were equilibrated to a constant temperature of 25 ± 1 °C in a Haake Model FK2 constant-temperature bath. The light intensity was determined at 436 nm using Reinecke's salt[21] and at 355 nm using ferric oxalate.[22] Emission quantum yield measurements were carried out using either the Spex Fluorolog spectrofluorometer or a Hitachi Perkin-Elmer Model 650-40 fluorescence spectrophotometer and deduced by comparison to $[Ru(bpy)_3]^{2+}$, having a known quantum yield of 0.042 at λ_{ex} = 436 nm.[23] Corrected emission spectra were recorded with the Spex instrument.

Samples for lifetime and emission experiments were prepared in 9-mm-diameter glass cells as optically dilute solutions ($\sim 10^{-5}$ M) in 4:1 (v:v) ethanol:methanol, were freeze–pump–thaw-degassed for four cycles, and then were sealed under vacuum. Excited-state lifetimes were determined with two different systems. The first used a Molectron DL-200 tunable dye head pumped by the fundamental of a Molectron UV-400 nitrogen laser as a pulsed source for excitation at 460 nm. Emission decay was monitored at right angles by a 0.25-m monochrometer/PMT (Hamamatsu R446) combination. The PMT output was accumulated by a Tektronix 7912AD transient digitizer, and the results obtained for a series of pulses were collected and averaged by using a PDP 11/34 minicomputer. The second system was similar in design but consisted of a PRA LN1000 pulsed nitrogen laser coupled with a PRA LN 102 tunable dye head as the source and a LeCroy 6880A waveform transient digitizer as the data collector. In both systems stray excitation light was removed by placing a 2.5-cm dichromate solution filter between the sample and monochromator. Lifetimes were determined by least-squares fits of single exponential decays over at least 3 half-lives.[24,25] Temperature control for the temperature-dependent lifetime experiments was obtained by use of a Janis NDT-6 or a Cryo Industries Model EVT cryostat controlled by Lakeshore DRC-84C temperature controllers. For fitting procedures, the VAX 11/780 computer in conjunction with the RS/1 data manipulation program and the IBM PS/2 Model 60 microcomputer were used. The low-temperature emission spectral fits were performed with an algorithm described by Lumpkin.[26]

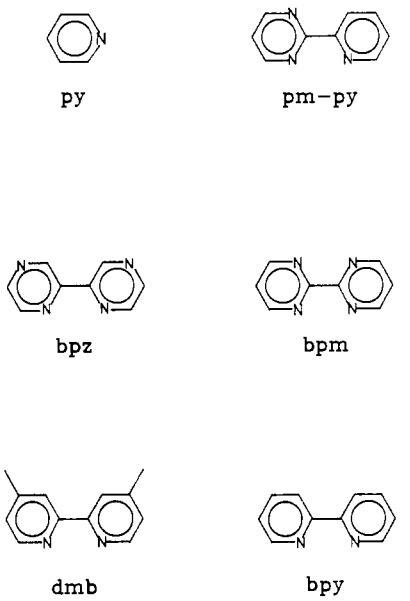

Figure 1. Polypyridyl ligands.

Proton nuclear magnetic spectra were obtained using a General Electric 300-MHz spectrometer. Mass spectrometry measurements were carried out using a Du Pont Model 21490 mass spectrometer.

Elemental analyses were carried out by Atlantic Microlabs, Inc., Norcross, GA.

Results

Preparation of Compounds. The structure and abbreviations of the polypyridyl ligands are shown in Figure 1. The ligand 2-(2′-pyridyl)pyrimidine (pypm) was prepared according to the procedures of Lafferty and Case[20] in an overall yield of approximately 10%. The preparations of $[Ru(pypm)_3]^{+2}$, $[Ru(pypm)_2(bpy)]^{2+}$, and $[Ru(bpy)_2(pypm)]^{2+}$ were carried out by methods reported for other $[Ru(bpy)_x(L–L)_{3-x}]^{2+}$ complexes,[15] where L–L = bpz or bpm, x = 0, 1, or 2. The preparation and properties of $[Ru(pypm)_3]^{2+}$ were published earlier,[27] but additional details are added here. In the present work, we also report an improved preparation of $[Ru(bpy)_2(py)_2]^{2+}$ from $Ru(bpy)_2CO_3$ which minimizes luminescent impurities. The preparation and characterizations of other bis(pyridine) complexes of the general formula $[Ru(L–L)_2(py)_2]^{2+}$, L–L = bpz, bpm, dmb, bpy–bpz,

(21) Wegner, E. E.; Adamson, A. W. *J. Am. Chem. Soc.* **1966**, *88*, 394.
(22) Allmand, A. J.; Webb, W. W. *J. Chem. Soc.* **1929**, 1518.
(23) Sullivan, B. P.; Salmon, D. J.; Meyer, T. J.; Peedin, J. *Inorg. Chem.* **1979**, *18*, 3369.
(24) (a) Caspar, J. V.; Meyer, T. J. *J. Am. Chem. Soc.* **1983**, *105*, 5583. (b) Caspar, J. V.; Meyer, T. J. *Inorg. Chem.* **1983**, *22*, 2444.
(25) Allsopp, S. R.; Cox, A.; Kemp, T. J.; Reed, W. J. *J. Chem. Soc., Faraday Trans. 1* **1978**, *74*, 1275.
(26) Lumpkin, R. S. Ph.D. Thesis, The University of North Carolina at Chapel Hill, 1987.
(27) Kawanishi, Y.; Kitamura, N.; Tazuke, S. *Inorg. Chem.* **1989**, *28*, 2968.

Table II. Half-Wave Potentials for Ruthenium(II) Complexes[a]

complex	oxidation	reduction					
	$E_{1/2}$	$E_{1/2}$ (1)	$E_{1/2}$ (2)	$E_{1/2}$ (3)	$\Delta E_{1/2}$[d]	$E_{1/2}^{3+/2+*}$[e]	$E_{1/2}^{2+*/+}$[f]
$[Ru(bpm)_3]^{2+}$[b]	+1.69	−0.91	−1.08	−1.28	2.60	−0.25	1.03
$[Ru(pypm)_3]^{2+}$	+1.48	−1.15	−1.32	−1.53	2.63	−0.52	0.85
$[Ru(bpy)(pypm)_2]^{2+}$	+1.41	−1.17	−1.36	−1.68	2.58	−0.54	0.78
$[Ru(bpy)_2(pypm)]^{2+}$	+1.35	−1.20	−1.49	−1.73	2.55	−0.56	0.71
$[Ru(bpy)_3]^{2+}$[b]	+1.27	−1.31	−1.50	−1.77	2.58	−0.72	0.68
2-(2-pyridyl)pyrimidine[c]		−2.07					
2,2′-bipyridine[c]		−2.18					
2,2′-bipyrimidine[c]		−1.80					

[a] V vs SSCE (error is ±0.02 V); 0.1 M TBAH/CH_3CN; SR = 200 mV/s; T = 23 ± 1 °C. [b] Ross, H. B.; Boldaji, M.; Rillema, D. P.; Blanton, C. B.; White, R. P. *Inorg. Chem.* **1989**, *28*, 1013. [c] Kawanishi, Y.; Kitamura, N.; Tazuke, S. *Inorg. Chem.* **1989**, *28*, 2968. [d] $\Delta E_{1/2} = E_{1/2}(\text{oxid}) - E_{1/2}(\text{red})$. [e] $E_{1/2}^{3+/2+*} = E_{1/2} - E_{em}$ (eV). [f] $E_{1/2}^{2+*/+} = E_{em}$ (eV) + $E_{1/2}$ (1).

referred to in this paper were described previously.[4]

Electronic Spectra. The visible–UV absorption assignments of pypm complexes along with those of $[Ru(bpy)_3]^{2+}$ and $[Ru(bpm)_3]^{2+}$ are listed in Table I. The assignments were made by comparison to the parent tris complexes and on the basis of the well-documented optical transitions in $[Ru(bpy)_3]^{2+}$, where the low-energy transition is assigned as a metal to ligand charge-transfer (MLCT) transition ($d\pi \rightarrow \pi_1^*$) and another transition located approximately 6000 cm^{-1} higher in energy is assigned as the second MLCT band ($d\pi \rightarrow \pi_2^*$).[28,29] The lowered symmetry removes the degeneracy of the π^* levels, which results in the appearance of broad MLCT bands often containing shoulders.

For mixed-ligand complexes, the interpretation becomes more complex, since there are multiple $d\pi \rightarrow \pi_1^*$ and $d\pi \rightarrow \pi_2^*$ transitions. However, as noted in Table I, the absorption maxima of the first MLCT ($d\pi \rightarrow \pi_1^*$) bands are similar in energy for the various complexes, which means that the $d\pi \rightarrow \pi_1^*$(bpy) and $d\pi \rightarrow \pi_1^*$(pypm) transitions cannot be separated from one another as observed for other analogous series.[3,15]

Electrochemical Properties. Redox properties are summarized in Table II. $E_{1/2}$ values were determined by cyclic voltammetry, $\Delta E_{1/2}$ values were calculated by taking the difference in the $E_{1/2}$ value for oxidation ($E_{1/2,ox} = E_{1/2}^{3+/2+}$) and the first $E_{1/2}$ value for reduction ($E_{1/2}(1) = E_{1/2}^{2+/+}$), $E_{1/2}^{3+/2+*}$ was determined by subtracting the excited-state luminescent energy in electronvolts (determined from the luminescence maximum at room temperature) from the $E_{1/2}$ value for oxidation ($E_{1/2}^{3+/2+*} = E_{1/2(ox)} - E_{em}$), and $E_{1/2}^{2+*/+}$ was determined by adding E_{em} in electronvolts and the $E_{1/2}(1)$ value ($E_{1/2}^{2+*/+} = E_{em} + E_{1/2}(1)$). The redox processes were reversible one-electron processes as indicated by ΔE_p values ($\Delta E_p = E_{p,ox} - E_{p,red}$) that ranged between 60 and 70 mV[30] and an i_a/i_c ratio near 1.

The $E_{1/2}$ values were predictable on the basis of modifications of the model suggested by Lever.[31] In the case here, pypm consists of two different heterocycles, py and pm. Thus, by deducing the contribution to $E_{1/2}$ from each component and summing over all components, one can predict the potentials fairly accurately according to eq 1, where $E_{py} = E_{1/2}([Ru(bpy)_3]^{3+/2+})/6$ for oxi-

$$E_{calc} = \sum_i a_i E_{py} + \sum_j b_j E_{pm} \qquad (1)$$

dations or $E_{1/2}([Ru(bpy)_3]^{2+/+})/6$ for reductions, $E_{pm} = E_{1/2}([Ru(bpm)_3]^{3+/2+})/6$ for oxidations or $E_{1/2}([Ru(bpm)_3]^{2+/+})/6$ for reductions, and a and b are the number of py or pm units. On the basis of the relationships in eq 1, the calculated $Ru^{3+/2+}$ potentials compared to the experimental values are $E_{1/2}([Ru(pypm)_3]^{3+/2+}) = 1.48$ V ($E_{calc} = 1.48$ V), $E_{1/2}([Ru(pypm)_2(bpy)]^{3+/2+}) = 1.41$ V ($E_{calc} = 1.41$ V), and $E_{1/2}([Ru(bpy)_2(pypm)]^{3+/2+}) = 1.35$ V ($E_{calc} = 1.34$ V). In like manner, $Ru^{2+/+}$ potentials are $E_{1/2}(1)([Ru(pypm)_3]^{2+/+}) = -1.15$ V ($E_{calc} = -1.09$ V), $E_{1/2}(1)([Ru(pypm)_2(bpy)]^{2+/+}) = -1.17$ V ($E_{calc} = -1.18$ V), and $E_{1/2}(1)([Ru(bpy)_2(pypm)]^{2+/+}) = -1.20$ V ($E_{calc} = -1.24$ V).

Table III. Room-Temperature Luminescence Maxima, Emission, and Photochemical Quantum Yields[a]

complex	$\lambda_{max,em}$[b,c]	ϕ_{em}[c]	ϕ_p[d]
$[Ru(bpy)_3]^{2+}$[e]	620[f]	0.062[f]	0.0021
$[Ru(bpy)_2(py)_2]^{2+}$	626	0.001	0.0059
$[Ru(dmb)_2(py)_2]^{2+}$	630	0.0046	0.025
$[Ru(bpm)_2(py)_2]^{2+}$	670	0.0098	0.048
$[Ru(bpz)_2(py)_2]^{2+}$	665	0.023	0.070
$[Ru(bpy)_2(bpz)]^{2+}$	710[g]	0.019[g]	1.7×10^{-4}
$[Ru(bpy)(bpz)(py)_2]^{2+}$	655	0.0093	8.8×10^{-4}
$[Ru(bpy)_2(bpm)]^{2+}$	710[g]	0.004[g]	3×10^{-4}
$[Ru(bpy)(pypm)_2]^{2+}$	636[f]	0.025[f]	0.0066
$[Ru(bpy)_2(pypm)]^{2+}$	649[f]	0.028[f]	0.0039
$[Ru(pypm)_3]^{2+}$	620[f]	0.018[f]	0.0078
$[Ru(bpm)_3]^{2+}$	639[g]	0.0028[g]	0.043

[a] $\lambda_{max,em}$ in nm (λ_{ex} is ±3 nm); ϕ_{em} (error is ±10%); ϕ_p (error is ±10%). [b] Corrected emission maximum, λ_{ex} = 436 nm. [c] In 4:1 EtOH:MeOH (v:v) at 298 K, except as indicated. [d] Quantum yield for ligand loss in CH_3CN containing 1 mM $[(n\text{-}C_4H_9)]Cl$. [e] Dressick, W. J. Ph.D. Thesis, University of North Carolina at Chapel Hill, 1961; p 51. [f] In acetonitrile. [g] In propylene carbonate.

$\Delta E_{1/2}$ values remained relatively constant, as shown in Table II. In the past it has been shown that this parameter varied in parallel with the excited-state to ground-state energy gap and parallels the energy of the $d\pi \rightarrow \pi^*$ transition.[31] By inference, this is the case here as well, since both $\Delta E_{1/2}$ and the MLCT energies remain relatively constant.

The excited-state redox potentials indicate that the metals can behave as both photooxidants and photoreductants. As photoreductants, the pypm complexes have approximately the same driving force ($E_{1/2}^{3+/2+*} \sim -0.5$ V) whereas as photooxidants, the potentials ($E_{1/2}^{2+*/+}$) vary in the order $[Ru(pypm)_3]^{2+} > [Ru(pypm)_2(bpy)]^{2+} > [Ru(bpy)_2(pypm)]^{2+}$. The near-constant value of $E_{1/2}^{3+/2+*}$ results from the similarity in shifts in $E_{1/2}^{3+/2+}$ with E_{em}, whereas for $E_{1/2}^{2+*/+}$, E_{em} changes more rapidly than $E_{1/2}^{2+/+}$ as the ligands are changed.

Room-Temperature Luminescence and Photosubstitution Properties. Emission maxima, emission quantum yields and photochemical substitution quantum yields for pypm and bis(pyridine) complexes are listed in Table III. For the bis(pyridine) complexes emission maxima in 4:1 ethanol:methanol fell in the range 626 nm for $[Ru(bpy)_2(py)_2]^{2+}$ to 670 nm for $[Ru(bpm)(py)_2]^{2+}$. The bis(pyridine) complexes were weak emitters at room temperature. Emission quantum yields varied from 0.023 for $[Ru(bpz)_2(py)_2]^{2+}$ to 0.001 for $[Ru(bpy)_2(py)_2]^{2+}$, which is over 1 order of magnitude less than the yield for $[Ru(bpy)_3]^{2+}$ (0.042).[32] The pypm complexes, on the other hand, were strong emitters. Corrected emission maxima in 4:1 ethanol:methanol ranged from 620 nm for $[Ru(pypm)_3]^{2+}$ to 649 nm for $[Ru(bpy)_2(pypm)]^{2+}$ and emission quantum yields varied from 0.018 for $[Ru(pypm)_3]^{2+}$ to 0.028 for $[Ru(bpy)_2(pypm)]^{2+}$.

Ligand-loss photochemical quantum yields were determined in acetonitrile in the presence of chloride ion. The substitution

(28) Felix, F.; Ferguson, J.; Gudel, J. A.; Ludi, A. *J. Am. Chem. Soc.* **1980**, *102*, 4096.
(29) Kober, E. M.; Meyer, T. J. *Inorg. Chem.* **1982**, *21*, 3967.
(30) Nicholson, R. S.; Shain, I. *Anal. Chem.* **1964**, *36*, 705.
(31) Lever, A. B. P. *Inorg. Chem.* **1990**, *29*, 1271.
(32) Rillema, D. P.; Mack, K. B. *Inorg. Chem.* **1982**, *21*, 3849.

Table IV. Emission Spectral Fitting Parameters in 4:1 EtOH/MeOH at 77 K[a]

complex	E_{00}	$\hbar\omega_M$	S_M	$\hbar\omega_L$	S_L	$\Delta\bar{\nu}_{1/2}$
$[Ru(bpy)_3]^{2+}$ [b]	17380	1400	0.95	400	1.1	575
$[Ru(bpy)_2(py)_2]^{2+}$	17370	1380	1.29	300	2.00	530
$[Ru(dmb)_2(py)_2]^{2+}$ [c]	17350	1380	1.00	300	2.05	600
$[Ru(bpm)_2(py)_2]^{2+}$ [d]	16710	1360	1.35	300	2.10	575
$[Ru(bpz)_2(py)_2]^{2+}$ [e]	16690	1325	0.96	300	1.70	575
$[Ru(bpy)_2(bpz)]^{2+}$ [b,f]	15650	1300	0.9	300	1.25	650
$[Ru(bpy)(bpz)(py)_2]^{2+}$	15650	1300	0.85	300	1.80	600
$[Ru(bpy)_2(bpm)]^{2+}$ [b]	16000	1350	1.23	400	1.35	900
$[Ru(bpy)(pypm)_2]^{2+}$	17330	1380	0.88	400	1.23	560
$[Ru(bpy)_2(pypm)]^{2+}$	17220	1360	0.82	400	1.35	615
$[Ru(pypm)_3]^{2+}$	17440	1380	0.92	400	1.05	580
$[Ru(bpm)_3]^{2+}$ [b,f]	16750	1400	1.2	400	1.15	725

[a] Temp (error is ±2°); E_{00}, in cm^{-1} (error is ±30 cm^{-1}); $\hbar\omega$, in cm^{-1} (error is ±10 cm^{-1}); S (error is ±20%); $\Delta\bar{\nu}_{1/2}$, in cm^{-1} (error is ±5%). [b] Data from ref 2. [c] 88 K. [d] 91 K. [e] 94 K. [f] In propylene carbonate.

in pypm complexes occurs with the loss of the ligand with the lowest π^* energy level,[4] as illustrated in eq 2. A stepwise process

$$[Ru(bpy)_2(pypm)]^{2+} \xrightarrow[CH_3CN]{h\nu,\ Cl^-} [Ru(bpy)_2(CH_3CN)Cl]^+ + pypm \quad (2)$$

which involves ring opening, addition of Cl^- to the vacant coordination site, loss of the now "monodentate" ligand, and its replacement by CH_3CN to form $[Ru(bpy)_2(CH_3CN)Cl]^+$ follows from previous mechanistic arguments.[1b] Photosolvation by CH_3CN does not appear to play a role since photosubstitution in acetonitrile requires the presence of Cl^-. The substitution quantum yields vary by a factor of 2 from 0.0039 for $[Ru(bpy)_2(pypm)]^{2+}$ to 0.0078 for $[Ru(pypm)_2]^{2+}$. In bis(pyridine) complexes, one pyridine is lost and replaced with Cl^- according to eq 3. The possible formation of $Ru(bpy)_2Cl_2$ was also con-

$$[Ru(bpy)_2(py)_2]^{2+} \xrightarrow{h\nu,\ Cl^-} [Ru(bpy)_2(py)Cl]^+ + py \quad (3)$$

sidered as a photosubstitution product, but there was no spectral evidence for its formation. This was reasonable since the presence of Cl^- in the coordination sphere of $[Ru(bpy)_2(CH_3CN)Cl]^+$ results in a very weak emitter with a short lifetime, diminishing the possibility of secondary photolysis. The values of the photosubstitution quantum yields indicate that rather marked changes in photolability exist for various bis(pyridine) complexes. The most stable complex $[Ru(bpz)(bpy)(py)_2]^{2+}$ had an observed photosubstitution quantum yield 2 orders of magnitude lower than the most photolabile, $[Ru(bpz)(py)_2]^{2+}$. From these observations, replacement of one bidentate polypyridyl ligand by another can have a profound effect on the photochemical and photophysical properties of the complexes.

Emission Spectral Fitting Parameters. The corrected emission spectra of $[Ru(pypm)_3]^{2+}$ at 77 K and $[Ru(bpz)_2(py)_2]^{2+}$ at 94 K are shown in Figure 2. In Figure 2 are also illustrated band shapes calculated from spectral fitting parameters described earlier.[25,33] The results of the emission spectral fits are summarized in Table IV. The emission profiles were analyzed by the two-mode, temperature-dependent Franck–Condon analysis based on the parameters E_{00}, S_M, $\hbar\omega_M$, S_L, $\hbar\omega_L$, and $\Delta\bar{\nu}_{1/2}$. E_{00} is the zero–zero energy, S_M and $\hbar\omega_M$ are respectively the average electron-vibrational coupling constant and vibrational spacing for seven to eight medium-frequency ν(polypyridyl) ring stretching modes, S_L and $\hbar\omega_L$ are the corresponding quantities for an average of a series of low-frequency modes, and $\Delta\bar{\nu}_{1/2}$ is the full width at half-maximum for the individual vibronic contributors. In the emission spectra, vibrational progressions can be seen at 80–90 K, giving good initial estimates for $\hbar\omega_M$. The quantity S_M can readily be estimated from peak heights of the first two components. Low-frequency progressions are not observed at 80–90 K, although they must be included to obtain satisfactory fits. Consequently, we have set $\hbar\omega_L$ equal to 300 cm^{-1} for bis(pyridine) complexes and 400 cm^{-1} for pypm complexes and varied S_L and $\Delta\bar{\nu}_{1/2}$ in order to obtain the best fits at low temperature.

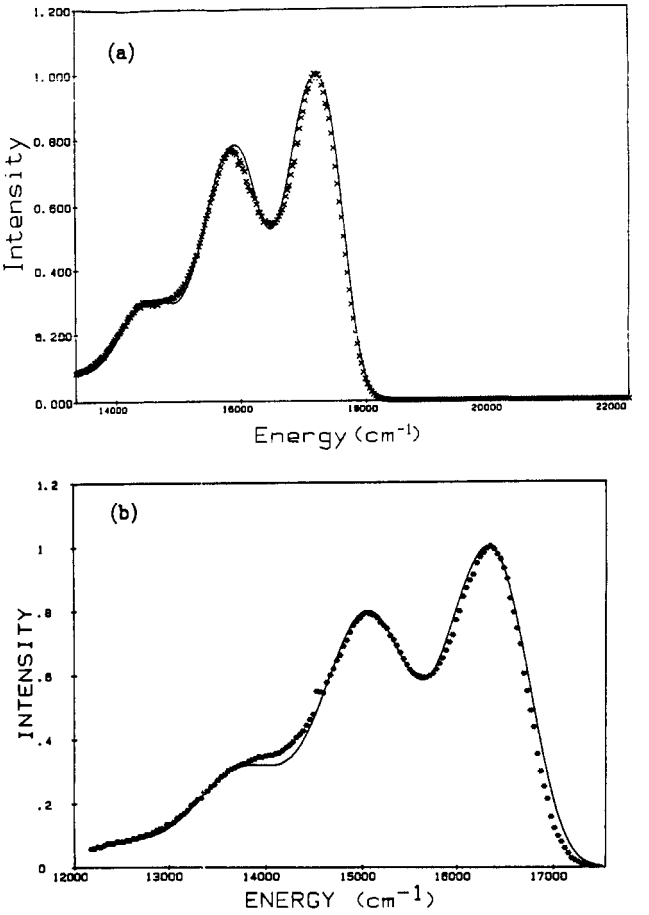

Figure 2. (a) Emission data (×) for $[Ru(pypm)_3]^{2+}$ at 77 K in a 4:1 C_2H_5OH:CH_3OH glass. (b) Emission data (✱) for $[Ru(bpz)_2(py)_2]^{2+}$ at 94 K in a 4:1 C_2H_5OH:CH_3OH glass. The computer fits (—) were generated by using the spectral parameters in Table IV.

Temperature-Dependent Lifetimes. Rate Constants for Excited-State Decay. Kinetic decay parameters are collected in Table V. Temperature-dependent lifetime data were fit to eq 4 by three

$$(\tau(T))^{-1} = (k_1 + k_2 \exp[-\Delta E_2/RT])/(1 + \exp[-\Delta E_2/RT]) \quad (4)$$

different techniques. These were a Gauss–Newton algorithm,[16a,24a] FLEXFIT[34] which allows variance in the variable plotted on the vertical axis, and an algorithm based on procedures outlined by Wentworth[35] which allows variance in both plotted variables. Since both τ and T were experimentally determined parameters,

(33) Caspar, J. V.; Westmoreland, T. D.; Allen, G. H.; Bradley, P. G.; Meyer, T. J.; Woodruff, W. J. *J. Am. Chem. Soc.* **1984**, *106*, 3492.
(34) Ramette, Richard W. Copyright, Carlton College, 1988.
(35) Wentworth, W. E. *J. Chem. Educ.* **1965**, *42*, 96, 162.

Table V. Kinetic Decay Parameters[a]

complex	τ_0[b]	k_1[c]	k_2	ΔE_2	k_r	k_{nr}
$[Ru(pypm)_3]^{2+}$	142	$(1.17 \pm 0.01) \times 10^6$	$(5 \pm 3) \times 10^{13}$	3340 ± 121	12×10^4	1.05×10^6
$[Ru(bpy)(pypm)_2]^{2+}$	388	$(1.70 \pm 0.04) \times 10^6$	$(1.3 \pm 0.2) \times 10^7$	483 ± 43	6.4×10^4	1.63×10^6
$[Ru(bpy)_2(pypm)]^{2+}$	405	$(1.18 \pm 0.02) \times 10^6$	$(2.2 \pm 0.4) \times 10^7$	550 ± 50	6.9×10^4	1.11×10^6
$[Ru(dmb)_2(py)_2]^{2+}$	20	$(7.1 \pm 0.6) \times 10^5$	$(4 \pm 5) \times 10^{15}$	3244 ± 82	23×10^4	0.48×10^6
$[Ru(bpz)_2(py)_2]^{2+}$	570	$(1.06 \pm 0.01) \times 10^6$	$(5 \pm 7) \times 10^{14}$	4212 ± 309	4×10^4	1.02×10^6
$[Ru(bpm)_2(py)_2]^{2+}$	40	$(8.7 \pm 0.03) \times 10^6$	$(3 \pm 17) \times 10^{17}$	4776 ± 1008	24×10^4	8.46×10^6
$[Ru(bpy)(bpz)(py)_2]^{2+}$	287	$(2.3 \pm 0.6) \times 10^6$	$(9 \pm 5) \times 10^6$	428 ± 198	3.2×10^4	2.26×10^6

[a] τ_0, in ns (error is ±5%); k in s^{-1}; ΔE in cm^{-1}. [b] In 4:1 C_2H_5OH:CH_3OH; T = 298 K; λ_{ex} = 436 nm. [c] In 4:1 C_2H_5OH:CH_3OH; T = 160–298 K; λ_{ex} = 436 nm.

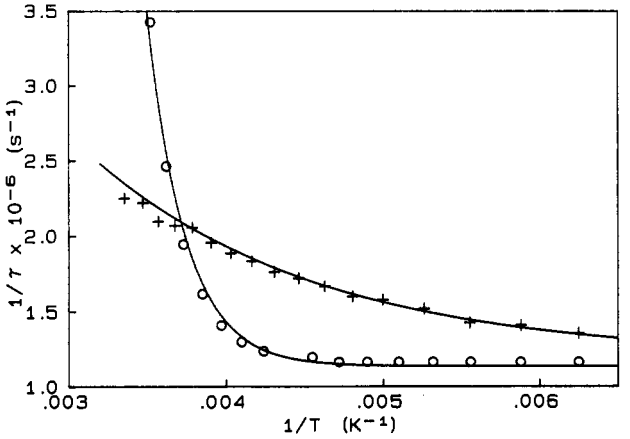

Figure 3. Comparison of the temperature-dependent lifetime data of $[Ru(pypm)_3)]^{2+}$ (○) and $[Ru(pypm)_2(bpy)]^{2+}$ (+) with a computer-generated fit using eq 4 and the parameters in Table V.

the latter approach is preferred and, as seen from the plots in Figure 3, gives satisfactory fits of the data.[36] The denominator in eq 4 is only necessary when ΔE_2 is small.[37] It should be noted that eq 4 forces all the temperature dependence into a single term. Previously, others[25] obtained fits to related data by using an equation with a second temperature-dependent exponential term. However, as shown in Figure 3, use of Wentworth's algorithm with eq 4 gives satisfactory fits to the experimental data.

The temperature-independent rate constant k_1 is the sum of the radiative (k_r) and nonradiative (k_{nr}) decay constants for the ^{3}MLCT state whose properties may represent an average of at least three low-lying states.[37,38] The complexes are sufficiently weak emitters that $k_{nr} \simeq 1/\tau_0$. Values of ηk_r were calculated from eq 5. In eq 5, η is the efficiency of populating the emitting state(s)

$$\phi_r = \eta k_r \tau \qquad (5)$$

following MLCT excitation. It is known that η is unity for $[Ru(bpy)_3]^{2+}$ over a wide range of wavelengths[39,40] which may be the case here as well. The values of k_r and k_{nr} are derived from room-temperature data, and k_1 is defined by measurements below 250 K. Values of k_r and k_{nr} determined at 280 K agree with those at 298 K within 10%. Even at room temperature the contributors to nonradiative decay by the temperature-dependent terms are small.

The photostabilities of $[Ru(bpy)_2(bpz)]^{2+}$ and $[Ru(bpz)(bpy)(py)_2]^{2+}$ are a subtle consequence of the effects of the ligand environment on electronic structure. In these asymmetrical complexes, the dd state is sufficiently destabilized relative to the low-lying MLCT state(s) that it is not significantly populated, especially at room temperature.

The experimental data in Table V can be summarized as follows. Within the series of complexes, k_{nr} and k_r differ by 1 order of magnitude or less, while k_2 varies by 10 orders of magnitude. Room-temperature lifetimes vary from 20 ns for $[Ru(dmb)_2(py)_2]^{2+}$ to 570 ns for $[Ru(bpz)_2(py)_2]^{2+}$. The ΔE_2 parameters vary from a low of 428 cm^{-1} for $[Ru(bpy)(bpz)(py)_2]^{2+}$ to a high of 4776 cm^{-1} for $[Ru(bpz)(py)_2]^{2+}$. In relative magnitude, the values k_{nr} exceed k_r by approximately 2 orders of magnitude for all of the complexes.

Discussion

The goal of the work was to continue to explore those factors at the molecular level which minimize the effects of low-lying dd states. The results of previous work[2] on $[Ru(bpy)_2(bpz)]^{2+}$ and $[Ru(bpy)_2(bpm)]^{2+}$ suggested that the emitting ^{3}MLCT state lies sufficiently below the dd state in these coordination environments that photochemical ligand loss is greatly suppressed. In this study we turned to the related complexes $[Ru(pypm)_3]^{2+}$, $[Ru(bpy)(pypm)_2]^{2+}$, $[Ru(bpy)_2(pypm)]^{2+}$, and $[Ru(bpy)(bpz)(py)_2]^{2+}$. The key element was to identify ligand combinations that would minimize photochemical ligand loss. On the basis of the lifetime and photochemical ligand-loss studies, this part of the study has been a success. The order of decreasing quantum yield toward ligand loss is $[Ru(pypm)_3]^{2+} > [Ru(bpy)(pypm)_2]^{2+} > [Ru(bpy)_2(pypm)]^{2+} > [Ru(bpy)(bpz)(py)_2]^{2+}$. There is extensive suppression of photochemical ligand loss in $[Ru(bpy)(bpz)(py)_2]^{2+}$ which opens up synthetic opportunities for the preparation of "photostable" light-induced electron-transfer systems based on "$[Ru(bpy)(bpz)]^{2+}$" as the chromophoric core.

The results of emission spectral fitting through the series of complexes give insight into excited-state structure. The data in Table IV reinforce earlier observations[2,32,5,33,37] which have shown that the degree of excited-state distortion depends upon the structure of the chromophoric ligand and, in a series of complexes having the same chromophoric ligand, on the energy gap between the ground and excited state. For the pypm series, E_{00} falls in the order $[Ru(pypm)_3]^{2+} > [Ru(bpy)(pypm)_2]^{2+} > [Ru(bpy)_2(pypm)]^{2+}$. For $[Ru(bpz)_2(py)_2]^{2+}$ and $[Ru(bpm)_2(py)_2]^{2+}$, E_{00} is approximately the same but there is a significant decrease in excited-state distortion for the bpz complex, as shown by the low S_M values. From a recent X-ray structure analysis the Ru–N bond distances in $[Ru(bpz)_3]^{2+}$ are comparable to those found in $[Ru(bpy)_3]^{2+}$.[41] Given the larger S_M values for the bpy complexes, this suggests that the equilibrium displacement between the ground and excited states is decreased with bpz as the acceptor ligand compared to bpy.

The relatively low value of S_M is shared with $[Ru(bpy)(bpz)(py)_2]^{2+}$, suggesting that the excited electron resides on the bpz ligand as expected. For the bpm complexes, there is a relatively high degree of distortion at bpm in the excited state. Because of the higher distortion in the excited state, there is more extensive overlap of the vibrational wavefunctions for ring-stretching acceptor modes between the ground and excited states. The greater vibrational overlap leads to a larger Frank–Condon factor than for the equivalent bpz complex, an enhanced rate constant for nonradiative decay, and a decreased excited-state lifetime.

(36) A comparison of the results obtained with the three curve-fitting techniques will be made in a review article on this topic.
(37) Kober, E. M.; Caspar, J. V.; Lumpkin, R. S.; Meyer, T. J. *J. Phys. Chem.* **1986**, *90*, 3722.
(38) (a) Hager, G. D.; Crosby, G. A. *J. Am. Chem. Soc.* **1975**, *97*, 7031. (b) Hipps, K. W.; Crosby, G. A. *Ibid.* **1975**, *97*, 7042.
(39) Demas, J. N.; Taylor, D. G. *Inorg. Chem.* **1979**, *18*, 3177.
(40) (a) Bensason, R.; Salet, C.; Balzani, V. *J. Phys. Chem.* **1976**, *80*, 2499. (b) Boletta, F.; Juris, A.; Mestri, M.; Sandrini, D. *Inorg. Chim. Acta* **1980**, *44*, 6175.
(41) Li, H.; Jones, D. S.; Schwind, D. C.; Rillema, D. P. *J. Crystallogr. Spectrosc. Res.* **1990**, *20*, 321.

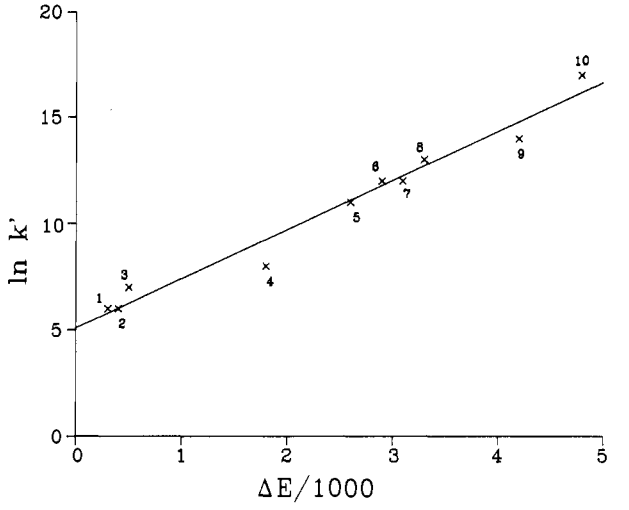

Figure 4. Barclay–Butler plot of ln k_2 vs ΔE_2. The correlation coefficient is 0.99, the slope is 2.9×10^{-3} cm, and the y intercept is 5.9. The data entries are (1) $[Ru(bpy)(bpz)(py)_2]^{2+}$, (2) $[Ru(bpy)_2(pypm)]^{2+}$, (3) $[Ru(bpy)_2(pypm)]^{2+}$, (4) $[Ru(bpy)_2(bpm)]^{2+}$, (5) $^{+}[Ru(bpm)^3]^{2+}$, (6) $^{+}[Ru(bpz)_3]^{2+}$, (7) $^{+}[Ru(bpy)_3]^{2+}$, (8) $^{+}[Ru(pypm)_3]^{2+}$, (9) $[Ru(bpz)_2(py)_2]^{2+}$, and (10) $[Ru(bpm)_2(py)_2]^{2+}$. The data were acquired in 4:1 (v:v) C_2H_5OH:CH_3OH, except for those cases noted with + which were acquired in propylene carbonate. The values of k_2 and ΔE_2 were recalculated from data in ref 2.

With the exception of two of the bpm complexes, the full width at half-maximum ($\Delta\bar{\nu}_{1/2}$) of the zero–zero vibronic component is fairly constant through the series of chromophoric ligands at 600 ± 50 cm^{-1}, which indicates that the outer-sphere reorganizational energy associated with the change in electron distribution between the excited state and ground state (χ_0) is fairly constant. This is reasonable given the common metal to ligand charge-transfer character of the excited states. In the spectral fitting procedure, it was not possible to deconvolute contributions from low-frequency modes and the solvent. The high values of $\Delta\bar{\nu}_{1/2}$ for two of the three bpm complexes may be a characteristic feature of bpm as the acceptor ligand and may be symptomatic of the greater contribution from low-frequency modes compared to the case of bpy, for example.

The results of temperature-dependent lifetime studies on a large number of polypyridyl complexes of ruthenium(II) and osmium(II) have been utilized to gain insight into excited-state structure and the dynamics of ligand-loss photochemistry via dd states. Additional temperature-dependent processes have been observed and attributed to population and decay of an MLCT state above the low-lying manifold of MLCT states first documented by Crosby et al.[38,42] From the temperature dependence of excited-state lifetimes, it can be proposed that two different kinetic limits exist. In the first $k_2 > 10^{12}$ s^{-1} and $\Delta E > 3000$ cm^{-1}; in the second $k_2 < 10^8$ s^{-1} and $\Delta E < 800$ cm^{-1}. The first limit and its associated kinetic parameters has been attributed to a nonradiative decay pathway involving irreversible thermal population and decay via a dd state. In the second limit, low-lying dd state(s) are populated to an insignificant extent at room temperature and an additional pathway involving nonradiative decay via a higher MLCT state(s) becomes apparent in the temperature-dependent data. In cases where the dd states contribute, their contribution masks that from the higher MLCT state(s). On the basis of this analysis, the kinetic decay parameters for $[Ru(pypm)_3]^{2+}$, etc. point to a temperature dependence dominated by thermal activation and decay via a dd state, whereas the parameters for $[Ru(bpy)(pypm)_2]^{2+}$, $[Ru(bpy)_2(pypm)]^{2+}$, and $[Ru(bpy)(bpz)(py)_2]^{2+}$ point to an additional activated decay channel via a higher energy MLCT state.

Similar changes in these kinetic parameters have been observed in mixed bpy–bpm and bpy–bpz complexes.[2] The effect was attributed there to changes in electronic structure that led to an increased energy gap to the dd state (ΔE_2), rendering it thermally inaccessible at room temperature. Although this interpretation may be correct, the ligand-loss quantum yields for the mono- and bis(pypm) complexes are appreciable and they merit further study.

A Barclay–Butler[43] plot (Figure 4) of ln k_2 vs ΔE_2 is linear ($r = 0.99$) with a y intercept of 5.1 and a slope of 2.9×10^{-3} cm. From the existence of a correlation of this type, it can be inferred that an increase in activation energy is accompanied by a greater density of vibrational levels at the point of barrier crossing, thus opening an increased number of reaction channels. Similar behavior has been noted for $[Ru(bpy)_3]^{2+}$,[24a] $[Rh_2(TMB)_4]^{2+}$, where TMB = 2,5-dimethyl-2,5-diisocyanohexane),[44] [*trans*-$Cr(NH_3)_2(NSC)_4]^-$,[45] and $[Cr(phen)_3]^{3+}$ [46] and rationalized in this way. Such effects are expected to be dominated by the low-frequency, collective dipole reorientation modes of the solvent.

An increase in the density of vibrational levels is expected for the MLCT → dd transitions.[24a] The solvent dipole environments around the complexes in the $(d\pi)^6$ ground or $(d\pi)^5(d\sigma^*)^1$ excited states are expected to be similar because there is no significant change in radial electronic distribution between states. The creation of a dipole in the MLCT excited state causes a change in solvent dipole orientations and stronger interactions with the solvent. This increases force constants and quantum spacings for the vibrational modes in the MLCT state which decreases the energy density of vibrational levels. In turn, this leads to an increase in the density of levels for the MLCT → dd transition. Although this argument may be correct qualitatively, it is hard to reconcile the magnitude of the preexponential terms (k_2) which reach 10^{17} s^{-1}. This problem needs to be analyzed in further detail.

The existence of the Barclay–Butler relationship (Figure 4) encompasses an extended series where the appearance of the temperature-dependent term (or terms) coincides with the appearance of ligand-loss photochemistry. For these cases this implies a common mechanism for the temperature-dependent term which is dominated by thermal population and decay through low-lying dd states. The few points where excited-state decay is dominated by an upper MLCT state (or states) (1–3 in Figure 4) appear to fall on the correlation. This may or may not be an experimentally significant observation given the different magnitudes of the quantities involved in the correlations. The suggested mechanisms for the two types of processes are certainly different.

Acknowledgment. We thank the Office of Basic Energy Sciences of the Department of Energy under Grants DE-FG05-84ER13263 and DE-FG05-86ER13633 and the National Science Foundation under Grant No. CHE-8719709 for support. We also thank Johnson-Matthey, Inc. for supplying on loan the $RuCl_3$ used in these studies.

(42) Komada, Y.; Yamauchi, S.; Hirota, N. *J. Phys. Chem.* **1988**, *92*, 6511.
(43) Barclay, I. M.; Butler, J. A. V. *Trans. Faraday Soc.* **1938**, *34*, 1445.
(44) Milder, S. J. *Inorg. Chem.* **1985**, *24*, 3376.
(45) Gutierrez, A. R.; Adamson, A. W. *J. Phys. Chem.* **1978**, *82*, 902.
(46) Allsopp, S. R.; Cox, A.; Kemp, T. J.; Reed, W. J.; Sostero, S.; Travero, O. *J. Chem. Soc., Faraday Trans. 1* **1980**, *76*, 162.